

ARTICLE

Received 17 Jan 2012 | Accepted 28 May 2012 | Published 26 Jun 2012

DOI: 10.1038/ncomms1931

Critical thickness for ferromagnetism in $\text{LaAlO}_3/\text{SrTiO}_3$ heterostructures

Beena Kalisky^{1,2}, Julie A. Bert¹, Brannon B. Klopfer², Christopher Bell¹, Hiroki K. Sato^{1,3}, Masayuki Hosoda^{1,3}, Yasuyuki Hikita¹, Harold Y. Hwang¹ & Kathryn A. Moler¹

In $\text{LaAlO}_3/\text{SrTiO}_3$ heterointerfaces, charge carriers migrate from the LaAlO_3 to the interface in an electronic reconstruction. Magnetism has been observed in $\text{LaAlO}_3/\text{SrTiO}_3$, but its relationship to the interface conductivity is unknown. Here we show that reconstruction is necessary, but not sufficient, for the formation of magnetism. Using scanning superconducting quantum interference device microscopy we find that magnetism appears only above a critical LaAlO_3 thickness, similar to the conductivity. We observe no change in ferromagnetism with gate voltage, and detect ferromagnetism in a non-conducting *p*-type sample. These observations indicate that the carriers at the interface do not need to be itinerant to generate magnetism. The ferromagnetism appears in isolated patches whose density varies greatly between samples. This inhomogeneity strongly suggests that disorder or local strain generates magnetism in a population of the interface carriers.

¹ Stanford Institute for Materials and Energy Sciences, SLAC National Accelerator Laboratory, Menlo Park, California 94025, USA. ² Department of Physics, Nano-magnetism Research Center, Institute of Nanotechnology and Advanced Materials, Bar-Ilan University, Ramat-Gan 52900, Israel. ³ Department of Advanced Materials Science, University of Tokyo, Kashiwa, Chiba 277-8561, Japan. Correspondence and requests for materials should be addressed to B.K. (email: beena@biu.ac.il).

For LaAlO_3 (LAO) grown on the TiO_2 -terminated surface of the $\{100\}$ face of SrTiO_3 (STO), the interfaces are conducting¹ above a 3-unit-cell (3 uc) thickness² of LAO. In such interfaces, called *n*-type, conductivity is attributed to interface electrons that migrate from the LAO into the conduction band of STO to solve the ‘polar catastrophe’ of an electric potential that would otherwise diverge with the thickness of the LAO^{1,3}. However, the density of carriers inferred from Hall transport is much less than the charge density needed to resolve the polar catastrophe, and is also nearly an order of magnitude less than the spectroscopic charge density found in X-ray studies^{4–6}. In addition, the interface is not conducting for any thickness of LAO grown on SrO termination layer (called *p*-type)^{1,7}, where an electronic reconstruction picture would predict that positively charged holes would migrate to the interface. These facts suggest that the polar catastrophe is an incomplete scenario: either competing atomic reconstructions occur to solve the potential divergence⁷, or many of the interface charge carriers must be localized^{4,6}, rather than mobile.

Magnetism at the interface has not been as extensively studied as conductivity. Magnetoresistance measurements^{8–10} suggest local magnetic moments, and bulk magnetization measurements find a variety of behaviours^{11,12}. In our previous work¹³, we directly imaged micron-scale ferromagnetic patches with scanning superconducting quantum interference device (SQUID) microscopy. Polarized neutron reflectometry measurements¹⁴ set an upper limit for surface magnetism that is at least 30 times smaller than that observed in bulk measurements, but is still higher than the values we measured by scanning SQUID¹³. Theoretical work suggests that interface electrons may^{15,16} or may not¹⁷ give rise to magnetism, and that the magnetism should be highly sensitive to oxygen¹⁸ and/or cation¹⁹ disorder.

To probe the relationship between interface conductivity and interface magnetism, we use scanning SQUID microscopy to image the magnetic landscape of a series of samples with different LAO thicknesses. We infer that electronic reconstruction, which only occurs in samples above a critical thickness, is necessary for

magnetism in LAO/STO. However, by imaging a non-conducting *p*-type sample and an electrostatically gated heterointerface, we found that tuning the itinerant carrier density does not modify the presence of magnetism. We therefore conclude that electronic reconstruction is necessary but not sufficient.

Results

Magnetic SQUID imaging of samples with varying LAO thickness. We use scanning SQUID microscopy^{20,21} to magnetically image many samples (Methods), primarily a series with varying LAO thickness. Figure 1a–d show representative examples of the magnetic landscapes for four thicknesses of the LAO layer. Our main observation is that a landscape of heterogeneous ferromagnetic patches similar to those shown in Fig. 1c,d appears in LAO/STO heterostructures starting at a LAO thickness of about 3 uc. Of 8 samples with LAO layer thicknesses from 3 to 15 uc, 7 have landscapes qualitatively similar to those in Fig. 1c,d, with strong sample-to-sample variability and heterogeneity, and two samples in this range (4 and 7 uc) show landscapes with a more dilute distribution of magnetic patches. The data on all 3 of the samples under 3 uc as well as 4 control samples (Methods) are consistent with the absence of magnetism below the critical thickness.

To characterize the individual ferromagnetic patches, we fit each one to a model of a point dipole with five free parameters: the dipole moment’s magnitude, azimuthal angle, inclination angle, and (x,y) position. In our measurement geometry (Fig. 1e,f), we scan the SQUID’s pickup loop about a micron (a sixth fitting parameter) above the sample surface²¹ while recording the total magnetic flux $\phi_s(x,y)$ through the pickup loop. The signal $\phi_s(x,y)$ is the local magnetic field of the sample integrated over the pickup loop area, with a sensitivity of $0.7 \mu\phi_0/\sqrt{\text{Hz}}$ (ref. 21), where ϕ_0 is 1 flux quantum, $\phi_0 = hc/2e$. An isolated micron- or submicron-scale ferromagnetic patch is conceptually similar to a small bar magnet with physical dimensions that are comparable to or smaller than the pickup loop. Figure 1g shows the flux $\phi_s(x,y)$ recorded while scanning the SQUID over an isolated magnetic patch. The size and intensity of the

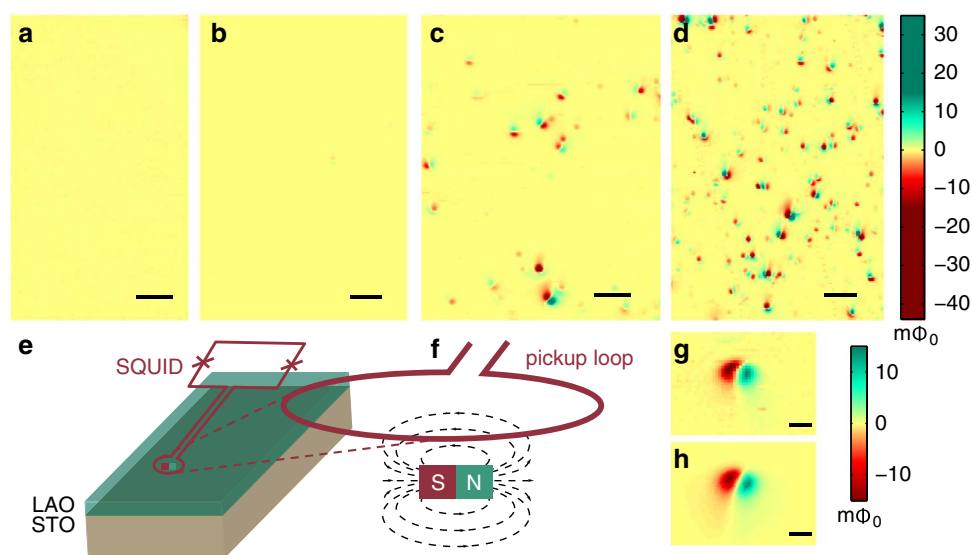


Figure 1 | Scanning SQUID images of the ferromagnetic landscape with increasing LAO thickness. (a–d) Typical scanning SQUID images of the LAO/STO surface, showing no ferromagnetic patches for (a) annealed STO and (b) 2 uc (unit cell) of LAO, and ferromagnetic patches for (c) 5 uc and (d) 10 uc of LAO, taken at 4K. Scale bar, 30 μm . (e,f) Sketch of magnetic imaging of a ferromagnetic patch with scanning SQUID. (e) Sketch of a SQUID probe with a 3 μm pickup loop near the surface of the sample. (f) Sketch of field lines from a ferromagnetic patch (conceptually shown here as a small bar magnet) captured in the pickup loop. (g) Image (data) of the flux through the pickup loop as the SQUID is scanned over a typical ferromagnetic patch. Scale bar, 10 μm . (h) Calculated image for an in-plane dipole whose moment is 7×10^7 Bohr magnetons and azimuthal angle, 20° , as determined by fitting the data in (g) to a point dipole model. Scale bar, 10 μm .

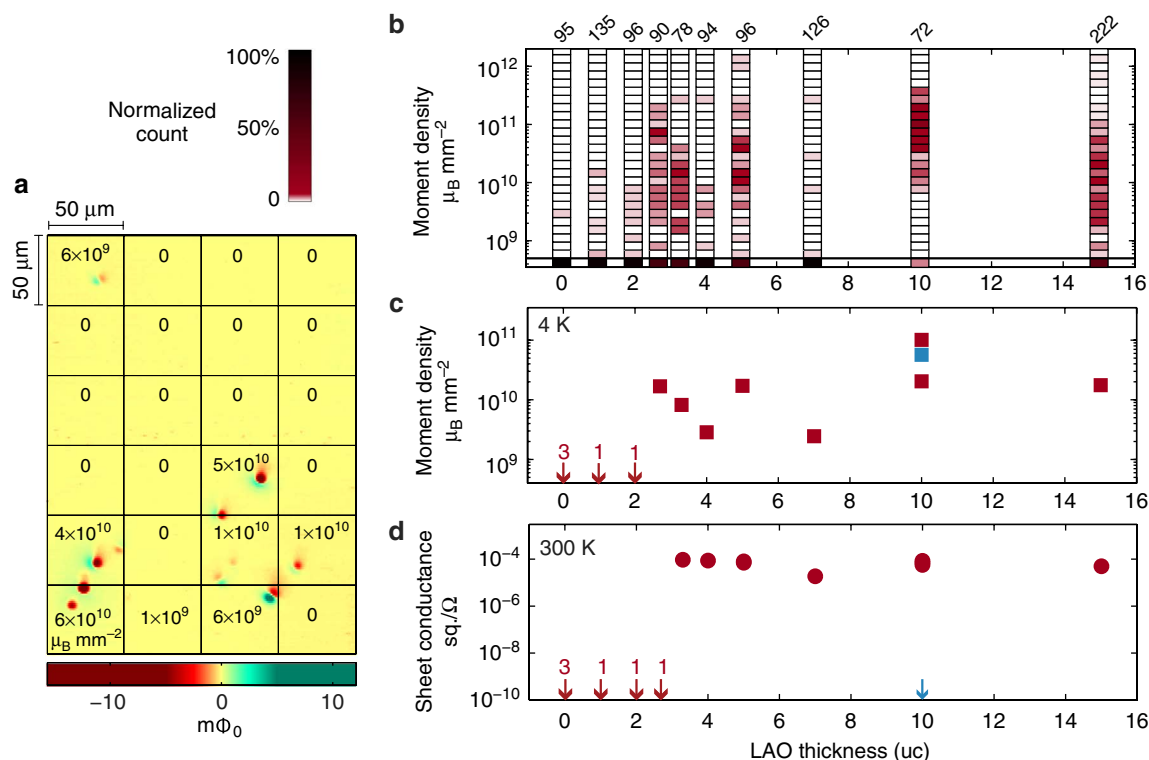


Figure 2 | Statistical distributions of magnetic moment density as a function of LAO thickness. (a) Large area scan measured at 4 K in the 5 uc sample divided into 50 $\mu\text{m} \times 50 \mu\text{m}$ squares demonstrates the inhomogeneous distribution of the ferromagnetic patches. The numbers are the moment density in $\mu_{\text{B}} \text{mm}^{-2}$ for each square. 8 out of 24 squares have non-zero moment. (b) Histograms of the moment densities for ten samples of varying thickness. For each sample, colour indicates the percentage of squares that have a particular moment density. The number at the top of each column represents the number of 50 μm squares measured in each sample. For example, in the 15 uc sample, we measured 222 squares of 50 $\mu\text{m} \times 50 \mu\text{m}$ and 75% of them had non-zero moment. Each histogram shows one representative sample per thickness. (c) Averaged moment density as a function of the thickness for TiO₂ terminated (red) and SrO terminated (blue). Off-scale values are marked by an arrow, which includes the number of samples for that thickness. (d) Sheet conductance at room temperature measured by the Van der Pauw method.

positive and negative lobes (green and red) depend strongly on the scan height as well as the characteristics of the patch itself, and the faint tails to the bottom of the dipole in the image are due to flux captured by the unshielded section of the leads to the pickup loop. Figure 1h shows a fitted image to compare with the data in Fig. 1g.

Heterogeneous distribution of ferromagnetic moments. We can check whether the magnitudes of the observed dipole moments are consistent with a scenario of interface magnetism. The distribution of patch sizes and magnitudes does not vary systematically as a function of thickness above the critical thickness. In terms of spatial extent, most of the patches are both isolated and resolution-limited in size as compared with our 3- μm pickup loop scanning at a height of about 1 μm , so their maximal area could be as large as $\sim 20 \mu\text{m}^2$. Most of them may be much smaller, although in some cases there seem to be neighbouring patches with different orientations or perhaps a much larger patch with internal domains. Under our measurement conditions, chosen to scan large areas on many samples, we can detect dipoles as small as $\sim 10^5$ Bohr magnetons (μ_{B}) (flux signal of $\sim 0.1 m\Phi_0$). The patches have a broad range of magnetic moments up to a few times $10^8 \mu_{\text{B}}$ with a typical value around $10^7 \mu_{\text{B}}$. Thus, we do not observe ferromagnetic patches that have a moment density per unit area much larger than $\sim 1 \mu_{\text{B}} \text{uc}^{-1}$ at the interface. The distribution of sizes and magnitudes of the patches, as well as the fact that the maximum size does not change with LAO thickness, are consistent with a scenario of interface magnetism.

A ferromagnetic patch at the interface would be nearly two-dimensional, and would therefore have large shape anisotropies

such that the magnetic moments would lie in plane. Indeed, the great majority of the magnetic moments do lie in plane or nearly so. Crystalline anisotropy may also have a role. The azimuthal angle of the ferromagnetic patches appears nearly random, although in some samples there may be four-fold symmetry of the azimuthal orientation, possibly owing to crystalline anisotropy. Because of this nearly random in-plane orientation, the vector sum of the moments in a typical data set such as in Fig. 1c,d would be much smaller than the sum of the magnitudes, making comparison to zero-field-cooled bulk measurements difficult. We note that the broad distribution of ferromagnetic patch sizes and shapes could give rise to odd behaviour when making sample-averaged measurements under various sample histories and conditions, and may explain at least some of the apparent inconsistency in previous reports of magnetism.

To quantify the spatially heterogeneous distribution of ferromagnetism that we observe in all of the ferromagnetic samples, and to enable comparison to sample-averaged probes of magnetism, we calculate the average moment density in 50 $\mu\text{m} \times 50 \mu\text{m}$ regions as well as in each sample (Fig. 2). For example, in the 5 uc sample (Fig. 2a), 16 out of the 24 regions shown in Fig. 2a had no detected magnetic moments larger than $2 \times 10^5 \mu_{\text{B}}$ (our sensitivity threshold). For comparison to other measurements and to theory, the highest density that we observe in any 50 $\mu\text{m} \times 50 \mu\text{m}$ region on any sample was $\sim 10^{12} \mu_{\text{B}} \text{mm}^{-2}$, which, if associated with Ti atoms at the interface, would correspond to $0.15 \mu_{\text{B}} \text{Ti}^{-1}$. Alternatively, if associated with the entire LAO layer in that sample, this density would correspond to 0.8emu cm^{-3} (taking 2 nm as the LAO layer thickness of a 5 uc sample) in a single 50 $\mu\text{m} \times 50 \mu\text{m}$ region. Most regions

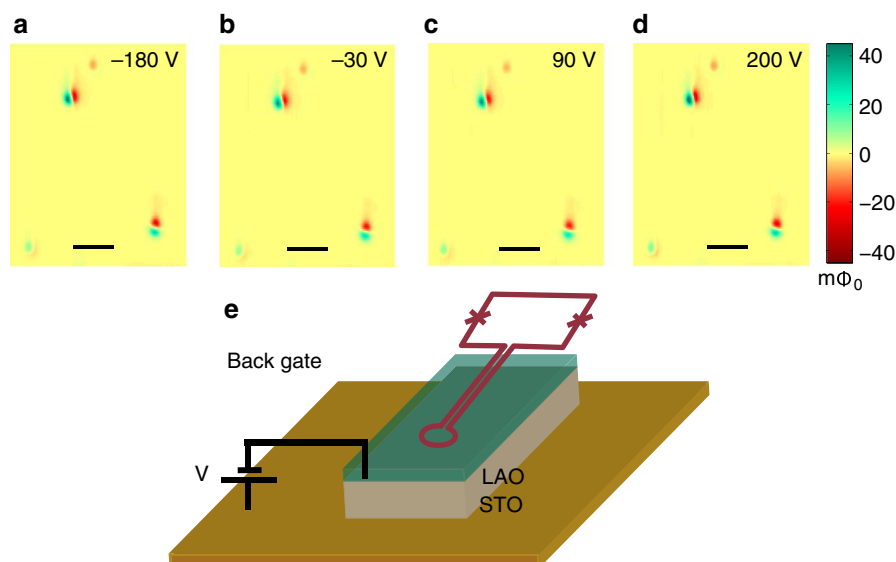


Figure 3 | The ferromagnetic patches do not change as a function of gate voltage. Scanning SQUID images repeatedly taken at 80 mK in a 5 uc *n*-type LAO/STO sample at back-gate voltage of -180 V (a) -30 V (b) 90 V (c) and 200 V (d). Scale bar, 20 μm . A sketch of the back-gate configuration is shown in (e).

had much lower density, which would give an even smaller signal in bulk or sample-averaged measurements.

Evolution of conductivity and magnetism with LAO thickness.

To compare the evolution of the conductivity and the magnetism, Fig. 2c,d show the average moment density (scalar) in each sample and the sheet conductance measured on the same samples as a function of LAO thickness. These data indicate a critical thickness of 3 uc for the appearance of ferromagnetic patches (the 2.7 uc sample is composed of 2 and 3 uc regions). In agreement with the literature, the heterointerface is insulating for LAO thicknesses ≤ 3 uc². These observations are also consistent with a number of measurements demonstrating a precursor of the metal-insulator transition in the orbital reconstruction and the spectroscopic appearance of Ti^{3+} occurring at 3 uc (refs 6,22), before macroscopic conductivity is observed above a percolation threshold²³.

Tuning the itinerant carrier concentration. To further probe the relationship between magnetism and conductivity, we tuned the conductivity of a 5 uc sample with a back gate^{24,25} (Fig. 3). This geometry allows for the application of a gate bias while preserving access to the sample surface by scanning SQUID. We found that the individual ferromagnetic patches do not change with gate voltage. Previous work showed that carrier concentration changes weakly with gating, while mobility changes rapidly²⁴. We also looked for magnetism in non-conducting LAO/STO (*p*-type)^{1,7} (Fig. 4) and found that a *p*-type LAO/STO interface (STO terminated by a single unit cell of SrO) exhibits strong heterogeneous magnetism similar to the *n*-type samples. This indicates that the TiO_2 termination layer, which is essential for conductivity, is not necessary for magnetism.

To summarize our main observation, magnetism appears only above a threshold LAO thickness that is similar to the critical thickness observed in conductivity studies. This supports a correlation between the appearance of magnetism and reconstruction of the interface. Other findings reported in this work (heterogeneity of ferromagnetism, sample-to-sample variability, magnetism in a non-conducting *p*-type interface, and independence of magnetism on gate voltage) all show that magnetism does not require the interface charge carriers to be mobile.

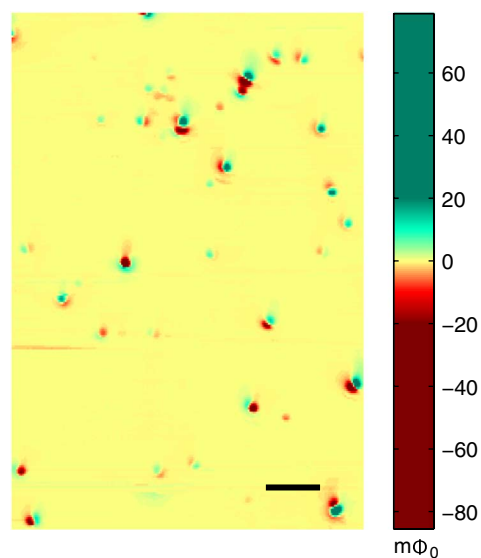


Figure 4 | Magnetic landscape in a *p*-type sample. Scanning SQUID image shows a typical ferromagnetic landscape in a 10 uc non-conducting SrO-terminated *p*-type LAO/STO sample at 4 K. Scale bar, 30 μm .

Discussion

Theoretical work on the possibility of magnetism in LAO/STO can be approximately classified in two categories. In one category, the origin can be attributed to the band structure itself. Density functional theory (DFT) applied to a perfect interface¹⁵ finds a number of nearly degenerate states, some of which have finite spin polarization on sites at and near the interface. In general, DFT predicts the occurrence of narrow, heavy electron mass sub-bands in the accumulation layer at the interface. Their propensity to localize in the presence of even small disorder has been suggested to account for the discrepancy between the measured Hall density and that found spectroscopically¹⁶. However, other theoretical work using dynamical mean-field theory does not suggest a stable magnetic ground state¹⁷. Whether localization could stabilize a spin-polarized state

(including for p -type interfaces), and the microscopic origin of the disorder potential, remain to be clarified.

A second category of theoretical approaches identifies cation or oxygen vacancies as a source of local moments¹⁹. In particular, a recent model finds that incorporating oxygen vacancies at the LAO/STO interface¹⁸ greatly enhances the tendency towards magnetism. While the results presented here cannot fully distinguish between these theoretical ideas, the importance of defects and disorder is clearly illustrated by both the sample-to-sample variability and by the heterogeneity within each sample, especially the existence of large regions (tens of microns) with little or no detectable ferromagnetism. This heterogeneity far exceeds that which can be attributed to magnetic impurities or spatial variations in the cation stoichiometry. Thus oxygen, strain and dislocations are all candidates for the relevant defect that tunes or seed the magnetism. The DFT work supports the importance of strain, if, as DFT suggests, there are moments at each site, the strain would change their separation²⁶ and therefore their coupling, possibly inducing ferromagnetism.

Nevertheless, the strong indications that the ferromagnetism reported here arises from the interface implies that it likely influences the superconductivity, which is known to exist at the interface below 300 mK (ref. 27). The presence of both ferromagnetism and strong spin-orbit coupling at the interface may favour a topological superconducting phase that would support Majorana fermions^{28,29}. These results suggest the exciting possibility that the tuning from non-ferromagnetic to ferromagnetic may also tune the local superconductivity from conventional to exotic.

Methods

Sample growth. LaAlO₃/SrTiO₃(100) samples were prepared by growing a certain number of unit cells (uc) of LaAlO₃ on commercial TiO₂-terminated {001} STO substrates. The growth process is as follows²⁴: The LaAlO₃ was deposited at 800 °C with an oxygen partial pressure of 1.3×10^{-5} mbar, after a pre-anneal at 950 °C with an oxygen partial pressure of 6.7×10^{-6} mbar for 30 min. The samples were cooled to 600 °C and annealed in a high-pressure oxygen environment (0.4 bar) for 1 h.

The LaAlO₃ thicknesses measured in this study are nominally 1, 2, 2.7, 3.3, 4, 5, 7, 10 and 15 uc, as calibrated by *in-situ* reflection high-energy electron diffraction during growth. Another 10 uc sample was grown on a SrO-terminated SrTiO₃ to create the p -type interface.

Control samples. Control samples measured in this study are: LaAlO₃ (100) as purchased, SrTiO₃ (100) as purchased, SrTiO₃ (100) annealed in the same conditions described for the thickness series above (defined as 0 uc), SrTiO₃ annealed in a different chamber (post-annealed in 1×10^{-3} bar for 60 min at 600 °C).

Although we tried to avoid magnetic contamination, small contamination while handling the samples is always possible³⁰ and could be responsible for the presence of an occasional dipole in the thinner samples: the low frequency of dipoles observed in these samples is consistent with the level of magnetism we find in other nonmagnetic samples and we attribute it to extrinsic contamination effects³⁰. On two samples, 1 with 5 uc of LAO and 1 with 15 uc of LAO, we saw several larger dipole moments, in the range of 2×10^8 – 2×10^9 μ_B . However, we are confident that these were not truly part of the LAO/STO heterostructure. To check whether they might be nanoparticles or dust contaminating the surface, we attempted to move them by scanning with the SQUID in contact with the sample and were successfully able to do so, unlike the vast majority of the smaller patches. To rule out contamination as a source of the magnetic signal, we tested the local elemental composition with CAMECA NanoSIMS on two areas in the 15 uc sample. The Al and Ti used as references behaved as expected, and Cr, Mn, Ni, Co, Ru did not appear, with an upper limit of 1–10 p.p.m. The samples show some weak magnetic features, such as rare weak dipoles, and in some cases, a weak magnetic landscape on a length scale of many tens of microns. These features are close to our resolution threshold, and are consistent with images we have seen on other nonmagnetic samples.

References

- Ohtomo, A. & Hwang, H. Y. A high-mobility electron gas at the LaAlO₃/SrTiO₃ heterointerface. *Nature* **427**, 423–426 (2004).
- Thiel, S., Hammerl, G., Schmehl, A., Schneider, C. W. & Mannhart, J. Tunable quasi-two-dimensional electron gases in oxide heterostructures. *Science* **313**, 1942–1945 (2006).

- Schlom, D. G. & Mannhart, J. Oxide electronics: interface takes charge over Si. *Nat. Mater.* **10**, 168–169 (2011).
- Sing, M. *et al.* Profiling the interface electron gas of LaAlO₃/SrTiO₃ heterostructures with hard X-Ray photoelectron spectroscopy. *Phys. Rev. Lett.* **102**, 176805 (2009).
- Zhou, K. J. *et al.* Localized and delocalized Ti 3d carriers in LaAlO₃/SrTiO₃ superlattices revealed by resonant inelastic X-ray scattering. *Phys. Rev. B* **83**, 201402 (2011).
- Takizawa, M., Tsuda, S., Susaki, T., Hwang, H. Y. & Fujimori, A. Electronic charges and electric potential at LaAlO₃/SrTiO₃ interfaces studied by core-level photoemission spectroscopy. *Phys. Rev. B* **84**, 245124 (2011).
- Nakagawa, N., Hwang, H. Y. & Muller, D. A. Why some interfaces cannot be sharp. *Nat. Mater.* **5**, 204–209 (2006).
- Brinkman, A. *et al.* Magnetic effects at the interface between non-magnetic oxides. *Nat. Mater.* **6**, 493–496 (2007).
- Dikin, D. A. *et al.* Coexistence of superconductivity and ferromagnetism in two dimensions. *Phys. Rev. Lett.* **107**, 056802 (2011).
- Ben S. M. *et al.* Anisotropic magnetotransport at the SrTiO₃/LaAlO₃ interface. *Phys. Rev. B* **80**, 140403 (2009).
- Li, L., Richter, C., Mannhart, J. & Ashoori, R. C. Coexistence of magnetic order and two-dimensional superconductivity at LaAlO₃/SrTiO₃ interfaces. *Nat. Phys.* **7**, 762–766 (2011).
- Ariando *et al.* Electronic phase separation at the LaAlO₃/SrTiO₃ interface. *Nat. Commun.* **2**, 188 (2010).
- Bert, J. A. *et al.* Direct imaging of the coexistence of ferromagnetism and superconductivity at the LaAlO₃/SrTiO₃ interface. *Nat. Phys.* **7**, 767–771 (2011).
- Fitzsimmons, M. R. *et al.* Upper Limit to Magnetism in LaAlO₃/SrTiO₃ Heterostructures. *Phys. Rev. Lett.* **107**, 217201 (2011).
- Pentcheva, R. & Pickett, W. E. Charge localization or itineracy at LaAlO₃/SrTiO₃ interfaces: hole polarons, oxygen vacancies, and mobile electrons. *Phys. Rev. B* **74**, 035112 (2006).
- Popovic, Z. S., Satpathy, S. & Martin, R. M. Origin of the two-dimensional electron gas carrier density at the LaAlO₃ on SrTiO₃ interface. *Phys. Rev. Lett.* **101**, 256801 (2008).
- Chan, C. K., Werner, P. & Millis, A. J. Magnetism and orbital ordering in an interacting three-band model: a dynamical mean-field study. *Phys. Rev. B* **80**, 235114 (2009).
- Pavlenko, N., Kopp, T., Tsybal, E. Y., Sawatzky, G. A. & Mannhart, J. Magnetic and superconducting phases at the LaAlO₃/SrTiO₃ interface: the role of interfacial Ti 3d electrons. *Phys. Rev. B* **85**, 020407 (2012).
- Elfmov, I. S., Yunoki, S. & Sawatzky, G. A. Possible path to a new class of ferromagnetic and half-metallic ferromagnetic materials. *Phys. Rev. Lett.* **89**, 216403 (2002).
- Gardner, B. W. *et al.* Scanning superconducting quantum interference device susceptometry. *Rev. Sci. Instrum.* **72**, 2361–2364 (2001).
- Huber, M. E. *et al.* Gradiometric micro-SQUID susceptometer for scanning measurements of mesoscopic samples. *Rev. Sci. Instrum.* **79**, 053704 (2008).
- Salluzzo, M. *et al.* Orbital reconstruction and the two-dimensional electron gas at the LaAlO₃/SrTiO₃ interface. *Phys. Rev. Lett.* **102**, 166804 (2009).
- Nishimura, J., Ohtomo, A., Ohkubo, A., Murakami, Y. & Kawasaki, M. Controlled carrier generation at a polarity-discontinued perovskite heterointerface. *Jpn. J. Appl. Phys.* **43**, 1032 (2004).
- Bell, C. *et al.* Dominant mobility modulation by the electric field effect at the LaAlO₃/SrTiO₃ interface. *Phys. Rev. Lett.* **103**, 226802 (2009).
- Ben S. M., Ron, A., Palevski, A. & Dagan, Y. Shubnikov De Haas oscillations in SrTiO₃/LaAlO₃ interface. *Phys. Rev. Lett.* **105**, 206401 (2010).
- Bark, C. W. *et al.* Tailoring a two-dimensional electron gas at the LaAlO₃/SrTiO₃ (001) interface by epitaxial strain. *Proc. Natl Acad. Sci. USA* **108**, 4720–4724 (2011).
- Reyren, N. *et al.* Superconducting interfaces between insulating oxides. *Science* **317**, 1196–1199 (2007).
- Sau, J. D., Lutchyn, R. M., Tewari, S. & Das Sarma, S. Generic new platform for topological quantum computation using semiconductor heterostructures. *Phys. Rev. Lett.* **104**, 040502 (2010).
- Michaeli, K., Potter, A. C. & Lee, P. A. Superconducting and ferromagnetic phases in SrTiO₃/LaAlO₃ oxide interface structures: possibility of finite momentum pairing. *Phys. Rev. Lett.* **108**, 117003 (2012).
- García, M. A. Surface magnetism in ZnO/Co₃O₄ mixtures. *J. Appl. Phys.* **107**, 043906 (2010).

Acknowledgements

We thank Chuck Hitzman for his help with the NanoSIMS measurements, and Martin E. Huber for assistance in SQUID design and fabrication. We thank A. J. Millis, J. Mannhart, S. Raghu, and G. A. Sawatzky for helpful discussions. This work was primarily supported by U.S. DOE, Division of Materials Sciences, under Award No. DE-AC02-76SF00515. B.K. acknowledges support from FENA-MARCO contract

No. 0160SMB958. The CAMECA NanoSIMS was acquired with support from NSF ECCS-0922648.

Author contributions

Measurements: B.K. and J.A.B. Analysis: B.K. and B.B.K. with ideas developed with H.Y.H. and K.A.M. Sample growth: H.K.S., C.B., M.H., Y.H. and H.Y.H. Manuscript preparation: B.K. and K.A.M., with input from all co-authors.

Additional information

Competing financial interests: The authors declare no competing financial interests.

Reprints and permission information is available online at <http://npg.nature.com/reprintsandpermissions/>

How to cite this article: Kalisky, B. *et al.* Critical thickness for ferromagnetism in LaAlO₃/SrTiO₃ heterostructures. *Nat. Commun.* 3:922 doi: 10.1038/ncomms1931 (2012).

Erratum: Critical thickness for ferromagnetism in LaAlO₃/SrTiO₃ heterostructures

Beena Kalisky, Julie A. Bert, Brannon B. Klopfer, Christopher Bell, Hiroki K. Sato, Masayuki Hosoda, Yasuyuki Hikita, Harold Y. Hwang & Kathryn A. Moler

Nature Communications 3:922 doi: 10.1038/ncomms1931 (2012); Published 26 Jun 2012; Updated 6 Nov 2012

The affiliation details for Brannon B. Klopfer are incorrect in this Article. The correct address for this author is given below.

Stanford Institute for Materials and Energy Sciences, SLAC National Laboratory, Menlo Park, California 94025, USA.